



# Controllable defects and electrical properties of nonstoichiometric $\text{Na}_{0.5-x}\text{Bi}_{0.5+x}\text{Bi}_2\text{Nb}_2\text{O}_9$ high temperature piezoceramics



Zhihang Peng<sup>a,\*</sup>, Xinghe Xing<sup>a</sup>, Yang Xiang<sup>a</sup>, Feng Cao<sup>a</sup>, Bo Wu<sup>b</sup>

<sup>a</sup> Science and Technology on Advanced Ceramic Fibers and Composites Laboratory, National University of Defense Technology, Changsha 410073, Hunan, PR China

<sup>b</sup> Sichuan Province Key Laboratory Materials and Devices Application, Chengdu University of Information Technology, Chengdu 610225, Sichuan, PR China

## ARTICLE INFO

### Article history:

Received 13 July 2017

Received in revised form

4 September 2017

Accepted 5 September 2017

Available online 6 September 2017

### Keywords:

Ceramics

Dielectric response

Ionic conduction

Piezoelectricity

Vacancy formation

## ABSTRACT

High temperature piezoelectric materials have attracted much attention owing to their potential applications for structural health monitoring and nondestructive evaluation in new jet engines, steam and nuclear plants. Nonstoichiometric  $(\text{Na}_{0.5-x}\text{Bi}_{0.5+x})\text{Bi}_2\text{Nb}_2\text{O}_9$  high temperature piezoceramics were prepared by a conventional solid-state sintering route. The microstructure, dielectric, DC resistivity and piezoelectric properties were investigated. Pure Aurivillius phase structure only existed in a narrow region ( $-0.02 \leq x < 0.02$ ). Moreover, the anisotropic grain morphologies were significantly restrained by increasing Bi contents. The oxygen vacancies were artificially tailored in nonstoichiometric compositions. The dynamic piezoelectricity as a function of the poling electric field was also studied and underlying physic mechanism was discussed.  $(\text{Na}_{0.48}\text{Bi}_{0.52})\text{Bi}_2\text{Nb}_2\text{O}_9$  ceramic has the large piezoelectric coefficient ( $d_{33} \sim 20.8 \text{ pC/N}$ ), high Curie-temperature ( $T_C \sim 796 \text{ }^\circ\text{C}$ ) and low thermal aging rate ( $< 10\% @ 700 \text{ }^\circ\text{C}$ ), indicating that it is a promising candidate for ultra-high temperature piezoelectric sensor applications.

© 2017 Elsevier B.V. All rights reserved.

## 1. Introduction

The aerospace, aircraft and nuclear power industries have an imperative demand for sensors which can operate at  $500 \text{ }^\circ\text{C}$  or higher for structural health monitoring and nondestructive evaluation in recent years [1–3]. Bismuth layer structural ferroelectrics (BLSFs) have some fascinating characterization, such as high Curie-temperature, large spontaneous polarization and fatigue free properties [4–6]. BLSFs have attracted much attention due to their potential applications for high temperature sensors and nonvolatile ferroelectric random-access memories.

BLSFs, as called Aurivillius type compounds, are a large family of ferro- and piezoelectric ceramics with the general formula  $(\text{Bi}_2\text{O}_2)^{2+}(\text{A}_{m-1}\text{B}_m\text{O}_{3m+1})^{2-}$  [7,8]. Sodium bismuth niobate,  $\text{Na}_{0.5}\text{Bi}_{2.5}\text{Nb}_2\text{O}_9$  (NBN), is a typical two-layered Aurivillius-type compound with a high Curie temperature of  $790 \text{ }^\circ\text{C}$  [9]. However, the piezoelectric coefficient  $d_{33}$  of ordinarily firing NBN ceramics is relatively low ( $\sim 10 \text{ pC/N}$ ) owing to the restriction of spontaneous polarization in  $a$ - $b$  planes [10]. Chemical modification is an effective way to improve the piezoelectric properties or tailor other electrical

properties for Aurivillius type ceramics or other perovskite structural ferroelectrics [11,12]. Ce, Ta multi-dopants improve the piezoelectric activity of NBN-based ceramics [13]. Though the rare-earth  $\text{Ce}^{3+}/\text{Ce}^{4+}$  ions can significantly improve the piezoelectric properties, cerium ions decrease the DC resistivity and deteriorate the stability of piezoelectric properties at high temperature owing to the introduction of extra oxygen vacancies [14,15]. On the other hand, it is well known that the variation of K/Na ratio in  $(\text{K}, \text{Na})\text{NbO}_3$  and Zr/Ti ratio in  $(\text{Ba}, \text{Ca})(\text{Zr}, \text{Ti})\text{O}_3$  perovskite ceramics causes enhanced materials properties owing to metastability of structures [16–18]. In the pseudo-perovskite structure of NBN-ceramic, the A-site cations consist of  $\text{Na}^+$  and  $\text{Bi}^{3+}$  ions, giving a chance to prepare the different Na/Bi ratio of NBN-based ceramics. Meanwhile, different chemical valance of  $\text{Na}^+$  and  $\text{Bi}^{3+}$  ions is expected to cause the non-stoichiometric defects in Na-rich and Bi-rich compositions. Furthermore, Homma reported the phase diagram of the binary system  $\text{Bi}_5\text{Nb}_3\text{O}_{15}$ - $\text{NaNbO}_3$ , but any electrical properties were not mentioned [19]. Therefore, it is of great interest to study the effects of Na/Bi ratio on microstructure and correlated materials properties in  $\text{Na}_{0.5}\text{Bi}_{2.5}\text{Nb}_2\text{O}_9$  ceramics.

In the present work, nonstoichiometric  $\text{Na}_{0.5-x}\text{Bi}_{0.5+x}\text{Bi}_2\text{Nb}_2\text{O}_9$  ceramics were prepared by the conventional solid-state sintering route. A study concerning the Na/Bi ratio and correspond evolution

\* Corresponding author.

E-mail address: [chemiepengzh@gmail.com](mailto:chemiepengzh@gmail.com) (Z. Peng).

on the microstructure, electrical properties and thermal depolarization behavior of  $\text{Na}_{0.5-x}\text{Bi}_{0.5+x}\text{Bi}_2\text{Nb}_2\text{O}_9$  ceramics was systematically investigated.

## 2. Material and methods

Nonstoichiometric  $\text{Na}_{0.5-x}\text{Bi}_{0.5+x}\text{Bi}_2\text{Nb}_2\text{O}_9$  ceramics, where the  $x = -0.05, -0.02, 0, +0.02$  and  $+0.05$  (abbreviated as NBN-5, NBN-2, NBN-0, NBN+2, NBN+5) were prepared by the conventional solid-state sintering route. The metal oxides or metal carbonates,  $\text{Bi}_2\text{O}_3$  (99.9%),  $\text{Nb}_2\text{O}_5$  (99.99%) and  $\text{Na}_2\text{CO}_3$  (99.8%) were used as starting raw materials. The raw materials were weighed and then milled by  $\text{ZrO}_2$  balls in ethanol for 24 h. The mixtures were dried and then calcined at  $850^\circ\text{C}$  for 4 h. The calcined powders were milled again in the same condition, and granulated with 8 wt% polyvinyl alcohol (PVA) as a binder. The powders were finally diepressed into disks with dimensions of  $\Phi 10\text{ mm} \times 1\text{ mm}$  at a press of about 200 MPa. The compacts were sintered at  $1050^\circ\text{C}$  for 2 h, after burning out the binder at  $650^\circ\text{C}$  for 4 h.

The crystal structure of sintered ceramics was determined by an X-ray diffractometer (X'Pert Pro MPD, Philips, Netherlands) employing  $\text{Cu-K}\alpha$  radiation ( $\lambda = 1.5418\text{ \AA}$ ) at a step of  $0.02^\circ$ . The bulk density of the ceramics was measured by the Archimedes method. The surface morphologies of the ceramics were observed using a field-emission scanning electron microscope (S4800, Hitachi, Japan). Both surfaces of sintered ceramics were ground and polished into  $\sim 0.5\text{ mm}$  thick, and then fired Ag paste at  $750^\circ\text{C}$  for 10 min as the electrodes. The dielectric behavior and impedance properties as a function of temperature were performed using an LCR analyzer (IM3536, Hioki, Japan) attached to a programmable furnace. Samples were poled in a silicon oil bath at  $170^\circ\text{C}$  under a selected DC electric field for 10 min. The DC resistivity was measured in the temperature range of  $200\text{--}650^\circ\text{C}$  at a heating rate of  $5^\circ\text{C}/\text{min}$ . At each measurement point, the temperature was holding for 15 min to establish thermal equilibrium. A high resistance meter (CHT3530-1, Hope Electronic Science and Technology Co., Ltd, China) was used to measure the resistance with various applied voltages from 200 to 1 V. The piezoelectric coefficient  $d_{33}$  was measured using a quasi-static  $d_{33}$  meter (YE2730A, Sinocera Piezotronics Inc., China). The electromechanical coupling coefficient,  $k_p$  and mechanical quality factor,  $Q_m$  were determined by the resonance method according to the IEEE standard. The thermal depoling behavior were conducted by annealing the poled ceramics for 1 h at high temperature, cooling to room temperature freely, measuring  $d_{33}$  values, and repeating the procedure up to  $900^\circ\text{C}$ .

## 3. Results and discussion

Fig. 1 shows the XRD patterns of NBN-based ceramics sintered at  $1050^\circ\text{C}$ . The main diffraction peaks were indexed according to the standard PDF card (JCPDS #54–1054,  $\text{Bi}_5\text{AgNb}_4\text{O}_{18}$ ). The highest intensity of diffraction peak is found to be (115) orientation, which is in agreement with the fact that the most intense reflections of BLSFs are all of the type  $(112m+1)$  [20]. However, some impurity phases were detected in Na-rich or Bi-rich regions. The  $\text{NaNb}_3\text{O}_8$  and  $\text{Nb}_2\text{O}_5$  phases were found in the NBN-5 ceramic. The  $\text{BiNbO}_4$  phase was found in Bi-rich compositions ( $x \geq 0.02$ ). It is determined that the pure Aurivillius type structure formed in a narrow compositional region. The formation of impurities is mainly attributed to the difference of electronic valence of  $\text{Na}^+$  and  $\text{Bi}^{3+}$  cations. Furthermore, it was found that the diffraction peaks shift to the higher angles with an increase of  $\text{Bi}^{3+}$  concentration, indicating a decrease of lattice parameters of NBN-based ceramics. Owing to the 6s lone pair electrons of  $\text{Bi}^{3+}$  cations [21], the Bi-O bonds are shorter and more covalence than Na-O bonds, leading to the

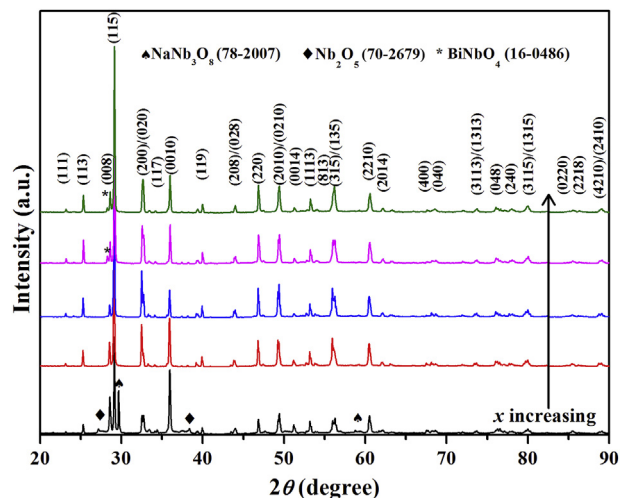


Fig. 1. XRD patterns of NBN-based ceramics sintered at  $1050^\circ\text{C}$  for 2 h.

rotation and tilting of  $\text{NbO}_6$  octahedra.

Fig. 2 presents the surface morphology of NBN-based ceramics sintered at  $1050^\circ\text{C}$ . The grains pack densely and few microvoids are observed, indicating that all ceramics have high density. It can be seen that the grain size obviously decreases with an increase of  $\text{Bi}^{3+}$  contents. In Na-rich region (NBN-5 and NBN-2 ceramics), the plain-like grain morphologies are detected, exhibiting a highly anisotropic crystallographic behavior. In Bi-rich region, however, rounded grains are observed. The average grain size (Fig. 2(f)) in the direction of diameter decreases from  $8.54$  to  $2.41\text{ }\mu\text{m}$ . The ratio of diameter size to thickness size ( $D/t$ ) drastically decreases from  $5.85$  to  $2.36$  with increasing  $\text{Bi}^{3+}$  contents, indicating a decrease of anisotropic morphologies of ceramic microstructure. The low melting temperature Na-based compounds could form the liquid phase and promote the grain growth in the Na-rich ceramics during the sintering process. It is concluded that the microstructure of NBN-based ceramics is evidently tailored by the different  $\text{Na}^+/\text{Bi}^{3+}$  ratio. The detailed element distribution of the NBN+2 ceramic is recorded. A typical EDS elemental mapping is shown in Fig. 3. The distribution of each element is random, suggesting that the composition of the NBN+2 ceramic is homogeneous. Though the secondary phase  $\text{BiNbO}_4$  was detected in the XRD pattern, no evident trail can be seen in Fig. 3, implying that the content of the  $\text{BiNbO}_4$  phase is relatively low in the NBN+2 ceramic.

The dielectric permittivity and loss values of NBN-based ceramics at 1 MHz are depicted in Fig. 4. The  $\epsilon_r$  values at room temperature increase from 126 to 164 with an increase of  $\text{Bi}^{3+}$  concentration. The dielectric constant peak  $\epsilon_{\text{max}}$  values increase from 934 to 1155 with increasing  $x$  values up to 0, but decrease to 794 with further increasing  $x$  values. The Curie temperature  $T_C$  as a function of  $x$  contents is also shown in the inset of Fig. 4. The  $T_C$  value of stoichiometric NBN ceramic is found to be  $791^\circ\text{C}$ , which is in agreement with other references [22,23]. It can be seen that the  $T_C$  value gradually increases from  $789$  to  $799^\circ\text{C}$  with increasing  $\text{Bi}^{3+}$  concentration. The 6s lone pair electrons of  $\text{Bi}^{3+}$  cations exhibit strong anisotropic behavior and stereo-chemical activity. As the structural distortion increases, the Curie temperature increases with increasing  $\text{Bi}^{3+}$  contents. The dielectric loss remains a relatively low value ( $\tan\delta \sim 2\%$ ) up to  $500^\circ\text{C}$ , and then gradually increases with an increasing temperature owing to the decrease of ceramic resistance.

Temperature dependent dielectric constants at selected frequencies of NBN-based ceramics are given in Fig. 5(a–e). A

Download English Version:

<https://daneshyari.com/en/article/5458201>

Download Persian Version:

<https://daneshyari.com/article/5458201>

[Daneshyari.com](https://daneshyari.com)